

HIGH EFFICIENCY LIGHT EMISSION THROUGH CARRIER LOCALIZATION IN ALGAN ALLOYS AND ACTIVE REGIONS: TOWARD VIABLE ULTRAVIOLET LIGHT SOURCES FOR THE OBJECTIVE FORCE WARRIOR

M. Wraback*, H. Shen, C.J. Collins, A.V. Sampath, G.A. Garrett, and W.L. Sarney
U.S. Army Research Laboratory, Sensors and Electron Devices Directorate, AMSRD-ARL-SE-EM
2800 Powder Mill Road, Adelphi, MD 20783

A.Y. Nikiforov and G.S. Cargill
Department of Materials Science and Engineering
Lehigh University, Bethlehem, PA

V. Dierolf
Department of Physics
Lehigh University, Bethlehem, PA

ABSTRACT

AlGa_N samples grown by plasma-assisted molecular beam epitaxy on sapphire (0001) substrates, with 20-50% Al content and without the use of indium, show intense room temperature photoluminescence that is significantly red-shifted, 200-400 meV, from band edge. This intense emission is characterized by a long room temperature lifetime (~300-400 ps) comparable to that seen in low defect density (~10⁸ cm⁻²) GaN. Room temperature monochromatic scanning cathodoluminescence images at the red-shifted peak reveal spatially non-uniform emission similar to that observed in In(Al)Ga_N alloys and attributed to compositional inhomogeneity. These observations suggest that spatial localization enhances the luminescence efficiency despite the high defect density (>10¹⁰ cm⁻²) of the films by inhibiting movement of carriers to nonradiative sites. Significant enhancement of this phenomenon has been obtained in a DH LED structure grown on a lower defect density AlGa_N template, with PL lifetime increased by nearly a factor of two, corresponding to a defect density in the mid-10⁷ cm⁻² range, and an internal quantum efficiency of ~ 30%. These results open the possibility of viable, low cost UV LEDs for bioagent detection and covert communication systems that provide protection and information at the individual soldier level and aid the development of survivability, lethality, and deployability of the Objective Force.

1. INTRODUCTION

Lightweight, low cost, uncooled optoelectronic sensors may be essential elements of future combat systems requiring more rapid and more lethal projection of force than that which can be presently achieved. III-nitride semiconductors are emerging materials for these

applications because of their wide bandgap, high breakdown voltage, and potential for operation in harsh, high temperature environments. Compact solid-state ultraviolet (UV) light emitters and detectors are essential for portable biodetection systems and non-line-of-sight (NLOS) covert communications. The inexpensive, rugged nature of these semiconductor UV sensors opens the possibility of a new class of disposable bioagent detectors and unattended ground sensors that may increase tactical options for battlefield commanders. The compactness, low power consumption, and lightness of these solid state devices as well as the systems in which they are incorporated will also contribute to the sustainability of the Objective Force by helping in the reduction of the logistics footprint. In addition, bioagent detection and covert communication systems based on these devices that provide protection and information at the individual soldier level will aid the development of survivability, lethality, and deployability of the Objective Force.

Aluminum gallium nitride (AlGa_N), with a bandgap tunable from 3.4 eV to 6 eV through variation of the relative Al and Ga content, has emerged as the material of choice for semiconductor optical sources in the 270 nm to 340 nm range crucial for bioagent detection and NLOS covert communication applications (Shaw et al., 2004, Radkov et al., 2004). One of the major problems that must be addressed before devices suitable for insertion in Army systems can be realized is that of reduced radiative efficiency due to nonradiative recombination associated with threading dislocations. Since low cost, native Ga_N or Al_N substrates are not yet available, most devices are fabricated on either sapphire or SiC substrates, with the resulting material quality limited by the high density of threading dislocations produced by the lattice mismatch between the III-nitride epilayers and these substrates. Enhanced radiative efficiency associated with carrier localization due to compositional fluctuations, often in the

Report Documentation Page				Form Approved OMB No. 0704-0188	
Public reporting burden for the collection of information is estimated to average 1 hour per response, including the time for reviewing instructions, searching existing data sources, gathering and maintaining the data needed, and completing and reviewing the collection of information. Send comments regarding this burden estimate or any other aspect of this collection of information, including suggestions for reducing this burden, to Washington Headquarters Services, Directorate for Information Operations and Reports, 1215 Jefferson Davis Highway, Suite 1204, Arlington VA 22202-4302. Respondents should be aware that notwithstanding any other provision of law, no person shall be subject to a penalty for failing to comply with a collection of information if it does not display a currently valid OMB control number.					
1. REPORT DATE 00 DEC 2004		2. REPORT TYPE N/A		3. DATES COVERED -	
4. TITLE AND SUBTITLE High Efficiency Light Emission Through Carrier Localization In Algan Alloys And Active Regions: Toward Viable Ultraviolet Light Sources For The Objective Force Warrior				5a. CONTRACT NUMBER	
				5b. GRANT NUMBER	
				5c. PROGRAM ELEMENT NUMBER	
6. AUTHOR(S)				5d. PROJECT NUMBER	
				5e. TASK NUMBER	
				5f. WORK UNIT NUMBER	
7. PERFORMING ORGANIZATION NAME(S) AND ADDRESS(ES) U.S. Army Research Laboratory, Sensors and Electron Devices Directorate, AMSRD-ARL-SE-EM 2800 Powder Mill Road, Adelphi, MD 20783; Department of Materials Science and Engineering Lehigh University, Bethlehem, PA				8. PERFORMING ORGANIZATION REPORT NUMBER	
9. SPONSORING/MONITORING AGENCY NAME(S) AND ADDRESS(ES)				10. SPONSOR/MONITOR'S ACRONYM(S)	
				11. SPONSOR/MONITOR'S REPORT NUMBER(S)	
12. DISTRIBUTION/AVAILABILITY STATEMENT Approved for public release, distribution unlimited					
13. SUPPLEMENTARY NOTES See also ADM001736, Proceedings for the Army Science Conference (24th) Held on 29 November - 2 December 2005 in Orlando, Florida.					
14. ABSTRACT					
15. SUBJECT TERMS					
16. SECURITY CLASSIFICATION OF:			17. LIMITATION OF ABSTRACT UU	18. NUMBER OF PAGES 7	19a. NAME OF RESPONSIBLE PERSON
a. REPORT unclassified	b. ABSTRACT unclassified	c. THIS PAGE unclassified			

presence of such high dislocation densities, was essential to the development of commercially successful blue InGaN-based light emitting diodes (LEDs). Specifically, it has been reported that the intense red-shifted photoluminescence (PL) peaks observed in InGaN alloys at room temperature result from the recombination of excitons localized at potential minima originating from large compositional fluctuations (Chichibu et al., 1997a, Chichibu et al., 1997b, Sun et al., 2004). Shorter wavelength emission, however, requires addition of Al to the active layers.

A similar localization effect in the AlGaIn material system, with the goal of producing efficient, deep UV LEDs without employing difficult-to-grow InAlGaIn quaternary alloys that tend to redshift the bandgap with increased indium incorporation, has been sought without success. Nevertheless, such localization phenomena have been reported for the quaternary InAlGaIn alloys having an InN mole fraction up to 20% and an AlN mole fraction up to 60% (Monroy et al., 2003, Ryu et al., 2002, Hirayama et al., 2002, Chen et al., 2004). The carrier localization observed in these quaternary materials is also attributed to indium segregation, resulting in enhanced luminescence at a peak wavelength significantly red-shifted (150-300 meV) with respect to the band edge. These red-shifts are much larger than those typically reported for AlGaIn alloys of comparable Al content (~10-50 meV), often attributed to emission from bandtails associated with alloy fluctuations and structural disorder (Cho et al., 2000, Bell et al., 2004, Kim et al., 2000). While AlGaIn on sapphire possesses long-lived low temperature PL (250-600 ps) from these localized states, the PL lifetimes drop to less than 20 ps at room temperature (Cho et al., 2000) due to thermally activated trapping and recombination at the large density of defect sites. In this paper, we report the first successful growth of high efficiency deep UV light emitting material with intense, long-lived (~300-400 ps) room temperature PL based on a spatial localization effect that enhances the luminescence efficiency by inhibiting movement of carriers to nonradiative sites, despite the high defect density of the AlGaIn epilayers on sapphire and without the effects of indium incorporation. In addition, we show that this phenomenon can be further enhanced in device structures grown on lower defect density AlGaIn templates, with nearly a doubling of the PL lifetime and internal quantum efficiency of ~ 30 %. These results open the possibility of viable, low cost UV LEDs for the Objective Force.

2. EXPERIMENTAL

AlGaIn samples having AlN mole fractions of 30-50% were investigated. All of the films consist of a 0.5 to 1.0 μm thick AlGaIn films deposited on *c*-plane sapphire

substrates by plasma-assisted molecular beam epitaxy (PAMBE). Prior to the growth of the epilayer, the sapphire substrate was nitridated and a 25 nm thick AlN buffer layer was deposited at the growth temperature, ~800 °C. A defect density of $\sim 10^{10} \text{ cm}^{-2}$ was estimated by TEM measurements. Variable temperature PL data was taken using a 244 nm cw-laser at an excitation power of ~0.5 mW. Reflectivity measurements were performed using a Perkin Elmer Lambda 19 UV/VIS/IR spectrometer system. Scanning cathodoluminescence (CL) images were taken with a 10 keV, 20 pA electron beam. Time-resolved experiments were performed using a 250 kHz Ti:sapphire regenerative amplifier-pumped optical parametric amplifier that produces ultrashort pulses frequency doubled to obtain a source of UV pulses tunable between 225 nm and 375 nm. Photoluminescence (PL) was measured with subpicosecond resolution using a novel PL downconversion technique (Garrett et al., 2002) that provides approximately one to two orders of magnitude better temporal resolution than standard ultraviolet time-resolved PL measurement techniques such as time-correlated photon counting (Bunea et al., 1999, Kwon et al., 2000) or use of a streak camera and spectrometer (Cho et al., 2000). In a downconversion experiment, the PL created by the radiative recombination of electron-hole pairs excited by an ultrafast ultraviolet pulse is time-resolved through gating of the PL in a

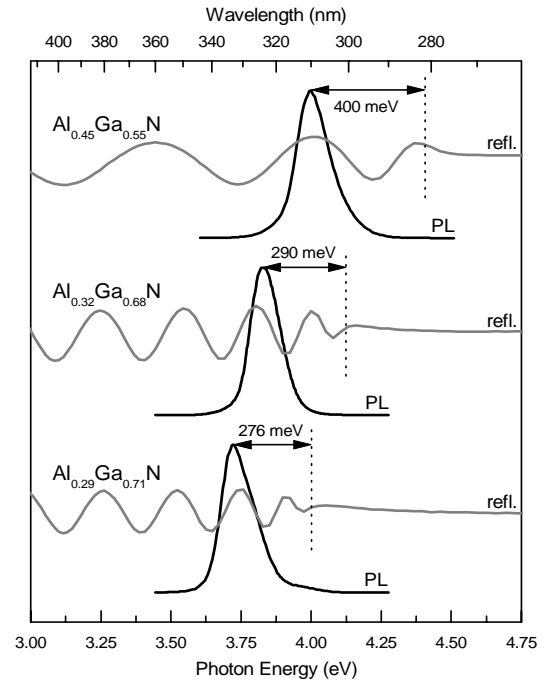


Fig. 1. Comparison of photoluminescence (PL) and reflectivity measurements (arb. scaled units) for $\text{Al}_x\text{Ga}_{1-x}\text{N}$ layers at room temperature. Vertical dashed lines indicate the location of the estimated band gap from photoreflectance studies.

nonlinear crystal with a synchronized ~ 800 nm pulse derived from the same source, the regenerative amplifier. Since the nonlinear process, downconversion, is nonresonant, it only occurs within the ~ 100 fs temporal slice of the luminescence coincident in time with the gating pulse. In this way, the time dependence of the PL can be mapped out with ~ 100 fs resolution by varying the timing of the gating pulse with respect to that of the excitation pulse using a mechanical delay line. While this experiment is quite similar to PL upconversion studies performed on infrared emitting materials (Shah, 1988), the lack of efficient detectors in the deep UV for detection of the upconverted UV PL dictates that downconversion of this PL to the visible is required.

3. ENHANCED ROOM TEMPERATURE LUMINESCENCE EFFICIENCY THROUGH CARRIER LOCALIZATION IN ALGAN ALLOYS

Room temperature PL data was collected and compared to reflectivity results for three different AlGaIn epitaxial layers (Fig. 1). The dotted lines represent the approximate band edge as determined by reflectivity and confirmed by photoreflectance measurements. The PL peak wavelengths are significantly red-shifted with respect to the band edge, and the PL intensities are orders of magnitude brighter than films with similar defect densities and only band edge emission. For these three epitaxial layers with aluminum percentages of 29%, 32%, and 45%, the red-shifts in PL from band edge are 276 meV, 290 meV, and 400 meV, respectively. To further investigate this effect, variable temperature PL spectra were taken from 10 K to 300 K on the $\text{Al}_{0.32}\text{Ga}_{0.68}\text{N}$ sample from Figure 1. At low temperature there are two distinct PL peaks, seen in Fig. 2. The red-shifted peak (3.89 eV, 319 nm) shows very bright emission at 10 K that decreases by a factor of ~ 7 as the temperature is increased from 10 to 300 K. The second peak (4.06 eV, 305 nm), associated with band edge emission, is seen at low temperature but its intensity rapidly decreases by greater than 3 orders of magnitude from 10 K to 300 K. Room temperature monochromatic scanning CL images ($2\ \mu\text{m} \times 2\ \mu\text{m}$) of the $\text{Al}_{0.32}\text{Ga}_{0.68}\text{N}$ film acquired at the red-shifted peak indicate that the emission is spatially nonuniform across the scanned area (Fig. 3), with feature sizes ranging from 50 to 500 nm in extent. The band edge peak had almost no measurable CL signal at room temperature.

To investigate the differences in these two PL peaks, time-resolved PL measurements were taken at room temperature on the $\text{Al}_{0.32}\text{Ga}_{0.68}\text{N}$ sample. Figure 4 shows the time evolution of the PL intensity measured at the band edge peak, Fig. 4(a), and the red-shifted peak, Figs. 4(b) and 4(c), after excitation with an ~ 290 nm laser pump pulse. TRPL data for the band edge emission peak

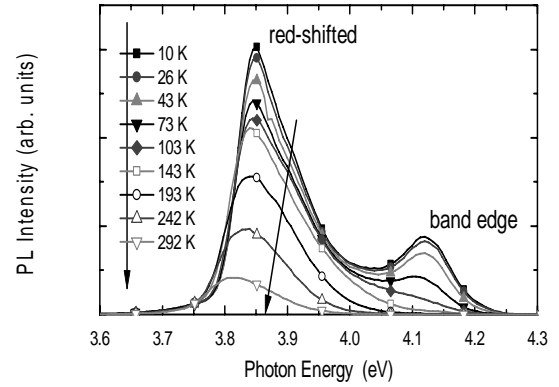


Fig. 2. Temperature-dependent PL spectra of the $\text{Al}_{0.32}\text{Ga}_{0.68}\text{N}$ film, excited with a 244 nm cw-laser at 0.5 mW, comparing red-shifted, 3.89 eV, and band edge, 4.06 eV, emission.

show a prompt, system-limited response at $t=0$ and an intensity dependent decay that saturates at higher pump intensity. These decays are characterized by half-lives from 15 to 25 ps for increasing pump intensities. TRPL data for the red-shifted peak, however, show intensity dependent initial rise times that achieve maxima at ~ 30 ps, 25 ps, and 5 ps for increasing pump fluence. Moreover, the semilog plot (Fig. 4c) shows that the red-shifted peak data possess a nearly intensity independent decay at low fluence ($< 50\ \mu\text{J}/\text{cm}^2$) that can be characterized by a half-life of ~ 300 ps and a dominant slow decay time in excess of 400 ps. At higher fluences a faster initial decay begins to develop, and the half-life

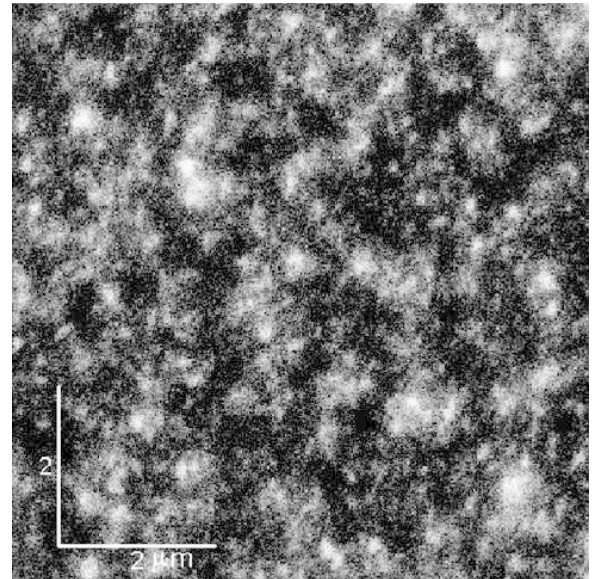


Fig. 3. Room temperature monochromatic scanning CL image for the $\text{Al}_{0.32}\text{Ga}_{0.68}\text{N}$ sample measured at the red-shifted emission, 3.84 eV.

drops to 270 ps. Similar behavior has been observed for each of the other samples discussed in Fig. 1, with high efficiency, long-lived PL found at wavelengths down to 310 nm for the highest Al content sample ($\text{Al}_{0.45}\text{Ga}_{0.55}\text{N}$).

The reflectivity data in Fig. 1 and accompanying photoreflectance studies (not shown) provide a measure of the band gap of these AlGaIn materials while indicating that the PL peaks are red-shifted with respect to the fundamental band gap. The spatial inhomogeneity of the red-shifted PL emission in Fig. 3 and the observation that the intensity of the band edge PL peak in Fig. 2 nearly vanishes at room temperature while that of the red-shifted peak decreases by less than one order of magnitude in raising the temperature from ~ 10 K to 300 K suggest both the presence of thermally activated transport of photogenerated carriers from the wider band gap AlGaIn matrix into localized states characterized by the longer wavelength emission and the suppression of nonradiative processes in these localized states. The room temperature TRPL data lends further credence to this interpretation. The slower band edge PL decays with increasing pump fluence, Fig. 4(a), imply that carriers are initially trapped in shallow localized states that are saturable at high carrier densities. When the transient PL data becomes independent of intensity at the highest pump fluence, the shallow states are strongly saturated and the half-life (25 ps) provides a measure of trapping at deep defect states most likely linked to the structural quality of the sample. These results are comparable to those obtained for typical AlGaIn alloys of similar defect density and Al content (Cho et al., 2000, Kim et al., 2000, Wraback et al., 2001). The localized states in these more conventional AlGaIn alloys at this Al content are characterized by bandtails with 20-30 meV width (Cho et al., 2000, Kim et al., 2000), as well as a large density of deep defect states. Although long lifetimes in bandtail states for such AlGaIn alloys have been reported at temperatures low enough to effect freeze-out of most nonradiative processes (Cho et al., 2000, Kim et al., 2000), at room temperature the carriers localized in the bandtails subsequently nonradiatively recombine through or are trapped in deep states associated with structural defects (Cho et al., 2000, Wraback et al., 2001) such that the PL decays have little or no spectral dependence. In contrast, Fig. 4(b) shows that the room temperature TRPL at the localized peak, 290 meV below the band gap, is strikingly different from its band edge counterpart. Since the reflectance data indicates that the pump pulse creates carriers primarily in the wider band gap AlGaIn matrix, the slow rise time corresponds to the transfer of carriers from the surrounding matrix to localized states that participate more readily in radiative than in nonradiative processes. As the carrier density increases, saturation of the localized states causes the transient PL signal at the red-shifted peak to achieve its maximum at earlier times, while the band edge TRPL decays become slower due to the filling

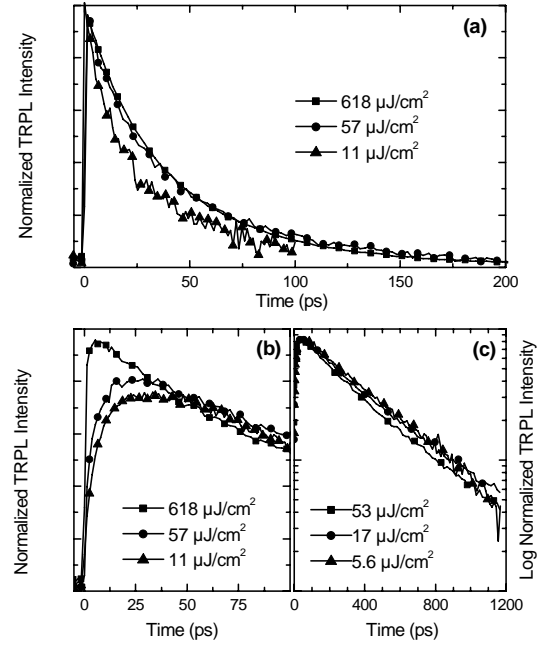


Fig. 4. Room temperature TRPL data from the $\text{Al}_{0.32}\text{Ga}_{0.68}\text{N}$ sample for the (a) band edge emission, 4.06 eV, and (b,c) localized emission, 3.84 eV, peaks.

of both these localized states and the more conventional bandtail states in the wider band gap AlGaIn matrix.

The 290 meV red-shift of the intense room temperature PL peak is comparable to those reported for InAlGaIn quaternary alloys (150-300 meV), which are attributed to compositional inhomogeneities related to indium incorporation (Monroy et al., 2003). The spatially non-uniform CL image in Fig. 3 is similar to those seen

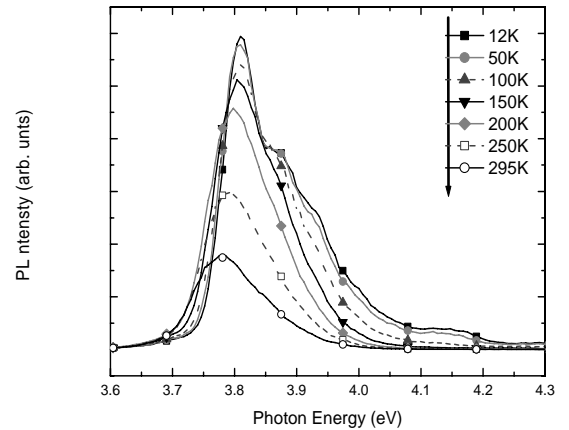


Fig. 5. Temperature-dependent PL spectra of the DH LED structure excited with a 0.5 mW, 244 nm cw-laser.

for both InAlGa_N quaternary alloys (Hirayama et al., 2002) and InGa_N ternary alloys (Chichibu et al., 1997b), implying that similar compositional inhomogeneities may exist in our AlGa_N samples, even in the absence of indium. The relative intensity independence of the dominant slow component of the TRPL decays obtained at the red-shifted peak (Fig. 4(c)) combined with the weak temperature dependence of the time-integrated PL for this peak suggest that these compositional inhomogeneities provide regions of smaller band gap that reduce nonradiative recombination by inhibiting movement of the carriers to defect sites that act as nonradiative recombination centers. The relative immunity of the carriers in these localized states from nonradiative processes associated with the large density of defects in the films ($\sim 10^{10} \text{ cm}^{-2}$) is clearly seen in the ~ 300 ps half-life and dominant ~ 400 ps PL decay time of the red-shifted peak at room temperature, which compares favorably with that obtained for high quality MOCVD-grown Ga_N on sapphire (~ 250 ps) for a dislocation density of $4 \times 10^8 \text{ cm}^{-2}$ (Kwon et al., 2000). This apparent reduction of defect density is commensurate with the average size and spacing of the bright spots in the CL image of Fig. 3.

One might expect that a further enhancement of radiative efficiency may be attained through reduction of dislocation and point defect densities in both the higher Al content matrix and the localized regions of the material. To this end, we have investigated this phenomenon in a double heterojunction (DH) LED structure deposited by MBE on a $1.8 \mu\text{m}$ -thick $\text{Al}_{0.46}\text{Ga}_{0.54}\text{N}$ template grown by HVPE on sapphire. This template has a dislocation density estimated in the mid- 10^9 cm^{-2} range. A $1 \mu\text{m}$ $\text{Al}_{0.42}\text{Ga}_{0.58}\text{N}:\text{Si}$ ($n \sim 5 \times 10^{18} \text{ cm}^{-3}$) current spreading layer was grown nearly lattice-matched atop the $\text{Al}_{0.46}\text{Ga}_{0.54}\text{N}$ template under conditions that inhibit localization. The active region consists of a lightly doped 100 nm $\text{Al}_{0.3}\text{Ga}_{0.7}\text{N}:\text{Si}$ ($n \sim 1 \times 10^{17} \text{ cm}^{-3}$) layer exhibiting localization. The structure is capped with a 10 nm $\text{Al}_{0.42}\text{Ga}_{0.58}\text{N}$ electron blocking layer. The p-type current spreading layers are omitted for the optical studies.

Figure 5 shows the variable temperature PL for this sample. The intensity of the PL from the localized states in the active region only drops by a factor of 3.3 when the temperature is raised from 12 K to room temperature, thus indicating significantly enhanced radiative efficiency (up to $\sim 30\%$ internal quantum efficiency) due to reduction of defects in this sample relative to the structures grown on sapphire. This result is also reflected in the observation that the CW PL from this DH LED structure is 3 to 4 times brighter at room temperature than that from the samples on sapphire. Further insight into this phenomenon can be gleaned from the room temperature, intensity dependent TRPL data in Fig. 6. In this case, the

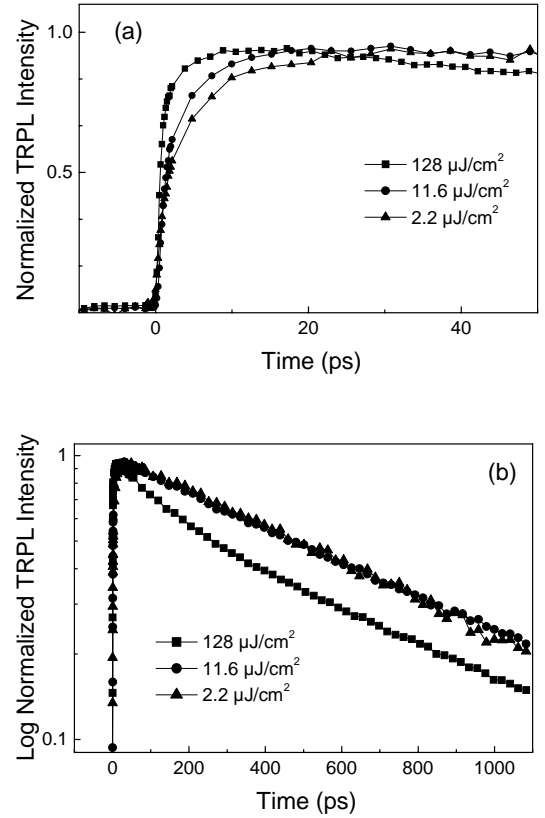


Fig. 6. Intensity dependent room temperature TRPL from the DH LED structure taken at the 330 nm peak corresponding to emission from localized states: (a) PL rise time; (b) PL decays.

pump pulse is tuned to 265 nm to include photogeneration of carriers in the barrier region of the structure. The decrease in PL rise time at the localized peak (330 nm) with increasing fluence (Fig. 6a) is consistent with similar data for the localized layer on sapphire (Fig. 4b), and is indicative of the more efficient transfer of carriers to the localized states with reduction of defect density. In addition, the PL lifetime (Fig. 6b) at low fluence ($< 20 \mu\text{J}/\text{cm}^2$) increases by nearly a factor of two in the DH LED structure relative to the localized layer on sapphire, with a half-life of ~ 500 ps, and a dominant decay time in excess of 700 ps. These times are comparable to those measured in high quality MBE Ga_N grown atop HVPE Ga_N templates with dislocation densities in the mid 10^7 cm^{-2} range (Sampath et al., 2004), suggesting that the further suppression of nonradiative recombination processes within and at the boundaries of the localized regions also contributes to the increased internal quantum efficiency in the DH LED structure. Finally, Fig. 6(b) shows a dramatic decrease in the half-life at the highest fluence ($128 \mu\text{J}/\text{cm}^2$) to 292 ps that is associated with the onset of a fast decay component. This drop in the PL

decay time, also hinted at in the high fluence data for the localized sample on sapphire (Fig. 4c), may be indicative of a decrease in the radiative lifetime at high carrier densities due to bimolecular recombination in the localized regions, which may be driven by enhanced carrier concentrations associated with the transfer of carriers from the AlGa_N matrix to the smaller localized regions and the suppression of nonradiative processes in these regions. This result offers promise for the development of lasers based on this localization phenomenon.

4. CONCLUSION

In conclusion, we have found that PAMBE-grown AlGa_N epitaxial layers on sapphire can exhibit intense room temperature PL emission red-shifted by ~ 200-400 meV with respect to the fundamental band gap. Spatial nonuniformity in room temperature scanning CL images and temperature dependent PL data characterizing this red-shifted peak imply that carriers generated in the wider band gap AlGa_N matrix undergo transport and trapping into localized states in a manner analogous to similar phenomena observed in In(Al)Ga_N alloys, for which this behavior is linked to compositional fluctuations. Room temperature TRPL measurements support this interpretation by providing a correlation between the decay time of the band edge PL and the rise time of the red-shifted PL. In addition, the long PL decay time of the red-shifted peak, which compares favorably with results for Ga_N in the $4 \times 10^8 \text{ cm}^{-2}$ defect range, suggests that we have developed a growth technique, without the use of indium, that encourages a spatial localization effect associated with compositional inhomogeneity in AlGa_N that enhances luminescence efficiency despite high defect densities by inhibiting the movement of carriers to nonradiative sites. Significant enhancement of this phenomenon has been obtained in a DH LED structure grown on a lower defect density AlGa_N template, with PL lifetime increased by nearly a factor of two, corresponding to a defect density in the mid- 10^7 cm^{-2} range, and an internal quantum efficiency of ~ 30%. These results open the possibility of viable, low cost UV LEDs for bioagent detection and covert communication systems that provide protection and information at the individual soldier level and aid the development of survivability, lethality, and deployability of the Objective Force.

ACKNOWLEDGEMENT

The authors would like to thank V. Dmitriev of TDI, Inc. for the AlGa_N template used for DH LED structure.

REFERENCES

- Bell, A., S. Srinivasan, C. Plumlee, H. Omiya, F.A. Ponce, J. Christen, S. Tanaka, A. Fujioka, and Y. Nakagawa, "Exciton freeze-out and thermally activated relaxation at local potential fluctuations in thick Al_xGa_{1-x}N layers", *J. Appl. Phys.*, Vol. 95, No. 9, pp. 4670-4674, May, 2004.
- Bunea, G.E., W.D. Herzog, M.S. Unlu, B.B. Goldberg, and R.J. Molnar, "Time-resolved photoluminescence studies of free and donor-bound exciton in GaN grown by hydride vapor phase epitaxy", *Appl. Phys. Lett.*, Vol. 75, No. 6, pp. 838-840, August, 1999.
- Chen, C.H., Y.F. Chen, Z.H. Lan, L.C. Chen, K.H. Chen, H.X. Jiang, and J.Y. Lin, "Mechanism of enhanced luminescence in In_xAl_yGa_{1-x-y}N quaternary epilayers", *Appl. Phys. Lett.*, Vol. 84, No. 9, pp. 1480-1482, March, 2004.
- Chichibu, S.F., T. Azuhata, T. Sota, and S. Nakamura, "Luminescences from localized states in InGa_N epilayers", *Appl. Phys. Lett.*, Vol. 70, No. 21, pp. 2822-2824, May, 1997a.
- Chichibu, S.F., K. Wada, and S. Nakamura, "Spatially resolved cathodoluminescence spectra of InGa_N quantum wells", *Appl. Phys. Lett.*, Vol. 71, No. 16, pp. 2346-2348, October, 1997b.
- Cho, Y.-H., G.H. Gainer, J.B. Lam, and J.J. Song, "Dynamics of anomalous optical transitions in Al_xGa_{1-x}N alloys", *Phys. Rev.*, Vol. B61, No. 11, pp. 7203-7206, March, 2000.
- Garrett, G. A., A. V. Sampath, C. J. Collins, F. Semendy, K. Aliberti, H. Shen, M. Wraback, Y. Fedyunin, and T. D. Moustakas, "Subpicosecond Luminescence Studies of Carrier Dynamics in Nitride Semiconductors Grown Homoepitaxially by MBE on Ga_N Templates", in *GaN and Related Alloys*, C. Wetzel, E.T. Yu, J.S. Speck, A. Rizzi, and Y. Arakawa, eds., *MRS Proceedings*, Vol. 743, pp. 349-354, 2003.
- Hirayama, H., A. Kinoshita, T. Yamabi, Y. Enomoto, A. Hirata, T. Araki, Y. Nanishi, and Y. Aoyagi, "Marked enhancement of 320-360 nm ultraviolet emission in In_xAl_yGa_{1-x-y}N with In-segregation effect", *Appl. Phys. Lett.*, Vol. 80, No. 2, pp. 207-209, January, 2002.
- Kim, H.S., R.A. Mair, J. Li, J.Y. Lin, and H.X. Jiang, "Time-resolved photoluminescence studies of Al_xGa_{1-x}N alloys", *Appl. Phys. Lett.*, Vol. 76, No. 10, pp. 1252-1254, March, 2000.
- Kwon, H.K., C.J. Eiting, D.J.H. Lambert, M.M. Wong, R.D. Dupuis, Z. Liliental-Weber, and M. Benamara, "Observation of long photoluminescence decay times for high-quality Ga_N grown by metalorganic chemical vapor deposition", *Appl. Phys. Lett.*, Vol. 77, No. 16, pp. 2503-2505, October, 2000.
- Monroy, E., N. Gogneau, F. Enjalbert, F. Fossard, D. Jalabert, E. Bellet-Amalric, L.S. Dang, and B.

- Daudin, "Molecular-beam epitaxial growth and characterization of quaternary III-nitride compounds", *J. Appl. Phys.*, Vol. 94, No. 5, pp. 3121-3127, September, 2003.
- Radkov, E., R. Bompiedi, A. M. Srivastava, A. A. Setlur, and C. A. Becket, "White light with UV LEDs", *Proc. SPIE Int. Soc. Opt. Eng.*, Vol. 5187, pp. 171-177, January, 2004.
- Ryu, M.-Y., C.Q. Chen, E. Kuokstis, J.W. Yang, G. Simin, and M. Asif Khan, "Luminescence mechanisms in quaternary $\text{Al}_x\text{In}_y\text{Ga}_{1-x-y}\text{N}$ materials", *Appl. Phys. Lett.*, Vol. 80, No. 20, pp. 3730-3732, May, 2002.
- Sampath, A.V., G.A. Garrett, C.J. Collins, P. Boyd, J. Choe, P.G. Newman, H. Shen, M. Wraback, R.J. Molnar, and J. Caissie, "Effect of Ga-rich growth conditions on the optical properties of GaN films grown by plasma-assisted molecular beam epitaxy", *J. Vac. Sci. Technol.*, Vol. B22, No. 3, pp. 1487-1490, May, 2004.
- Shah, J., "Ultrafast luminescence spectroscopy using sum frequency generation", *IEEE J. Quantum Electron.*, Vol. 24, No. 2, pp. 276-288, February, 1988.
- Shaw, G. A., A. M. Siegel, J. Model, and M. Nischan, "Field testing and Evaluation of a solar-blind UV communications link for unattended ground sensors" *SPIE Proceedings*, Vol. 5417, pp. 250-261, September, 2004.
- Sun, Y., Y.-H. Cho, E.-K. Suh, H.J. Lee, R.J. Choi, and Y.B. Hahn, "Carrier dynamics of high-efficiency green light emission in graded-indium-content InGa_N/Ga_N quantum wells: An important role of effective carrier transfer", *Appl. Phys. Lett.*, Vol. 84, No. 1, pp. 49-51, January, 2004.
- Wraback, M., F. Semendy, H. Shen, U. Chowdhury, D.J.H. Lambert, M.M. Wong, and R.D. Dupuis, "Time-resolved reflectivity studies of carrier dynamics as a function of Al content in AlGa_N alloys", *Phys. Stat. Sol. (a)*, Vol. 188, No. 2, pp. 807-810, 2001.